Supporting Information:

-

Plasmonic DNA-Origami Nanoantennas for Surface Enhanced Raman Spectroscopy

Paul Kühler[1], Eva-Maria Roller[2], Robert Schreiber[2], Tim Liedl[2], Theobald Lohmüller[1,], and Jochen Feldmann[1]*

[1]Photonics and Optoelectronics Group, Department of Physics and Center for NanoScience (CeNS), LMU München, Amalienstr. 54, Munich, 80799 (Germany)

[2] Department of Physics and Center for NanoScience (CeNS), LMU München, Geschwister-Scholl-Platz 1, Munich, 80539 (Germany)

Materials and Methods:

DNA origami folding. The DNA origami block was folded by mixing 10 nM of p8064 scaffold, 100 nM of each staple, 10 mM Tris, 1 mM EDTA (pH 8) and 14 mM $MgCl_2$. This mixture was heated up to 65 °C for 15 min and the slowly cooled down to 25 °C over 18 hrs. The folded DNA origami structures were then purified from excess staple strands by a 0.7 % agarose gel in 0.5x TBE buffer with 11 mM $MgCl_2$. The structures were extracted from the gel by using Freeze'N Squeeze spin columns (BioRad).

Concentration of AuNP colloids. The preparation of the DNA functionalized AuNPs (40 nm, BBI Solutions) followed with minor changes according to ref. 1. Firstly the colloid AuNP solution (50 mL, BBI Solutions, concentration c = 0.1 nM) of 40 nm diameter was concentrated. Therefore 20 mg of BSPP (Bis(p-sulfonatophenyl)phenylphosphine dihydrate dipotassium salt, Sigma-Aldrich) were added to the AuNPs and the solution was stirred over three nights. This step was followed by an addition of sodium chloride (5 M) till the color of the solution changed from red to bluish. The sodium chloride was added to screen the charge of the AuNP which leads to a decreasing distance of the particles. Hence it is possible to reach a higher concentration of AuNP after the solution was centrifugated at 1,600 rcf for 30 min and the supernatant was removed. The final concentration of sodium chloride in the AuNP solution was 240 mM. After resolving the AuNPs in 1 mL BSPP (2.5 mM) as well as 1 mL methanol, the solution was centrifuged again and the supernatant was removed afterwards. The concentrated AuNPs were dissolved in BSPP solution (1 mL, 2.5 mM, without sodium chlorid) and the concentration was determined to c(AuNP) = 10 nM by absorption measurement at a wavelength of 530 nm via UV-Vis spectroscopy (Nanodrop) (c = absorbance/(ε * d), with the molar extinction coefficient for 40 nm AuNP of ε = 8.42 * 109 and the pathlength d).

Modification of AuNPs with DNA. To conjugate the concentrated AuNPs with thiolated single stranded DNA (ssDNA, biomers.net) initially the thiolated ssDNA was incubated with TCEP (Tris(carboxyethyl)phosphine hydrochloride, Sigma-Aldrich; 20 mM final concentration) for 30 min. The AuNPs and thiolated ssDNA were afterwards mixed together in 0.5x TBE buffer at a ratio of AuNP:DNA = 1:5000. This solution was left for incubation overnight on a shaker. The protocol of Zhang *et al.*[2] was applied to achieve a better covering of the AuNPs with DNA. Therefore citrate buffer (pH = 3, 20 mM final concentration) was added to the solution. After 3 min the pH was raised again by adding 0.5x TBE buffer. To remove excessive unbound ssDNA strands the mixture was centrifuged over 100 kDa MWCO centrifugal filters (Amicon Ultra, Millipore, 10 min, 10,000 rcf). This filtering step was repeated eight times with adding of 400 µl 0.5x TBE buffer before each run.

Functionalization of DNA origami structures with AuNPs and transmission electron microscopy (TEM) grid preparation. The filtered DNA covered AuNPs were mixed together with the purified DNA origami structure in a ratio of 10 AuNPs per DNA origami structure. The solution was tumbled over 24 h at 22 °C. The DNA origami blocks with two attached 40 nm AuNPs were then purified from excess AuNPs via a 0.7 % agarose gel in 0.5x TBE buffer with 11 mM $MgCl_2$. The structures were again extracted from the gel by using Freeze'N Squeeze spin columns. To image and analyze the structures by TEM they were immobilized on a carbon-formvar-coated grid and stained with 1 % uranyl acetate. TEM measurements were performed using a JEOL JEM-1100 electron microscope.

Raman measurements and calculation of the enhancement factor (EF). Single-point Raman spectra were acquired with a T64000 triple grating Raman system (Horiba Scientific). The measurements were performed in air using the 568 nm line of an Argon/Krypton laser (Coherent) and a 100x MPlan N air objective (NA 0.9, Olympus). The acquisition time was 100 s per measurement and the laser power after the objective was measured to be 23.5 µW, yielding a power density at the focal position

of ~2.4 kW/cm². The combined Au and SYBR Gold fluorescence background was subtracted from the spectra to obtain the pure Raman signal.

Reference Raman measurements of the SYBR-gold were performed in bulk solution at 10000x concentration. The corresponding mass concentration in the commercial reagent was assumed to be ~10 mg/ml according Zipper *et al.*[3]. The SERS *EF* was determined by comparing the signals measured from single AuNP dimers with the intensity of the Raman signal from the bulk solution. The *EF* was calculated from the excitation power *P*, the integrated Raman intensity I_R (normalized with acquisition time), and the amount of molecules *N* contributing to the signal for the bulk SYBR-gold solution and for the nanoparticle origami, respectively:

$$\mathrm{EF} = \frac{\mathrm{I_{R,SERS}} \cdot \mathrm{P_{bulk}} \cdot \mathrm{N_{bulk}}}{\mathrm{I_{R,bulk}} \cdot \mathrm{P_{SERS}} \cdot \mathrm{N_{SERS}}}$$

I_R was taken from the SERS peak at 1365 cm^{-1}. P_{bulk} was 198 µW, P_{SERS} 23.5 µW as stated above. N_{bulk} is the calculated number of SYBR gold molecules in the confocal volume of the laser spot in the bulk measurement (~$9*10^7$). N_{SERS} was calculated as the fraction of the SYBR gold molecules in a DNA origami block (~25) which is located in the plasmonic hot spot between the AuNPs. The volume of the plasmonic hot spot was estimated as a tube with a diameter of 12 nm and a length of 6 nm according to FDTD calculations (SI: Fig. S7).

Dark-field scattering microscopy and spectroscopy. Scattering spectroscopy was performed in dark field configuration using an Epiplan Neofluar 100x air objective (NA=0.9, Zeiss) and an oil immersion dark field condenser with NA=1.2 (Zeiss). For illumination, a 100 W halogen lamp (Zeiss) and for spectral detection an Acton SP2500 spectrometer (Princeton Instruments) was used. Images were taken with a digital SLR camera (Panasonic).

Scanning electron microscopy (SEM). High-resolution images were taken with a Gemini Ultra Plus field emission scanning electron microscope (SEM) with a nominal resolution of 2 nm (Zeiss). The image information was collected by the in-lens detector at an electron accelerating voltage of 1 kV and a working distance of 1.6 mm. A 3 nm gold-palladium layer was sputtered on the sample prior to SEM investigation.

FDTD Simulations. FDTD simulations of Au nanoparticle dimers (particle diameter 40 nm, gap size 6 nm) were carried out using Lumerical FDTD solutions (Lumerical Solutions, Canada). Optical constant data tables were taken from Johnson and Christie for gold, and Palik for the dielectric surrounding (water as effective medium). With this setup, the calculations reproduced the experimentally measured scattering cross section dispersion. The simulation volume of 1.7 x 1.7 x 1.7 µm³ was confined with a stack of 64 perfectly matched layers with a reflection of 10^{-4}. Linear polarized light was injected with a total-field scattered-field source. Convergence was reached for a mesh size of 0.4 nm around the plasmonic particles.

Supporting Figure S1:

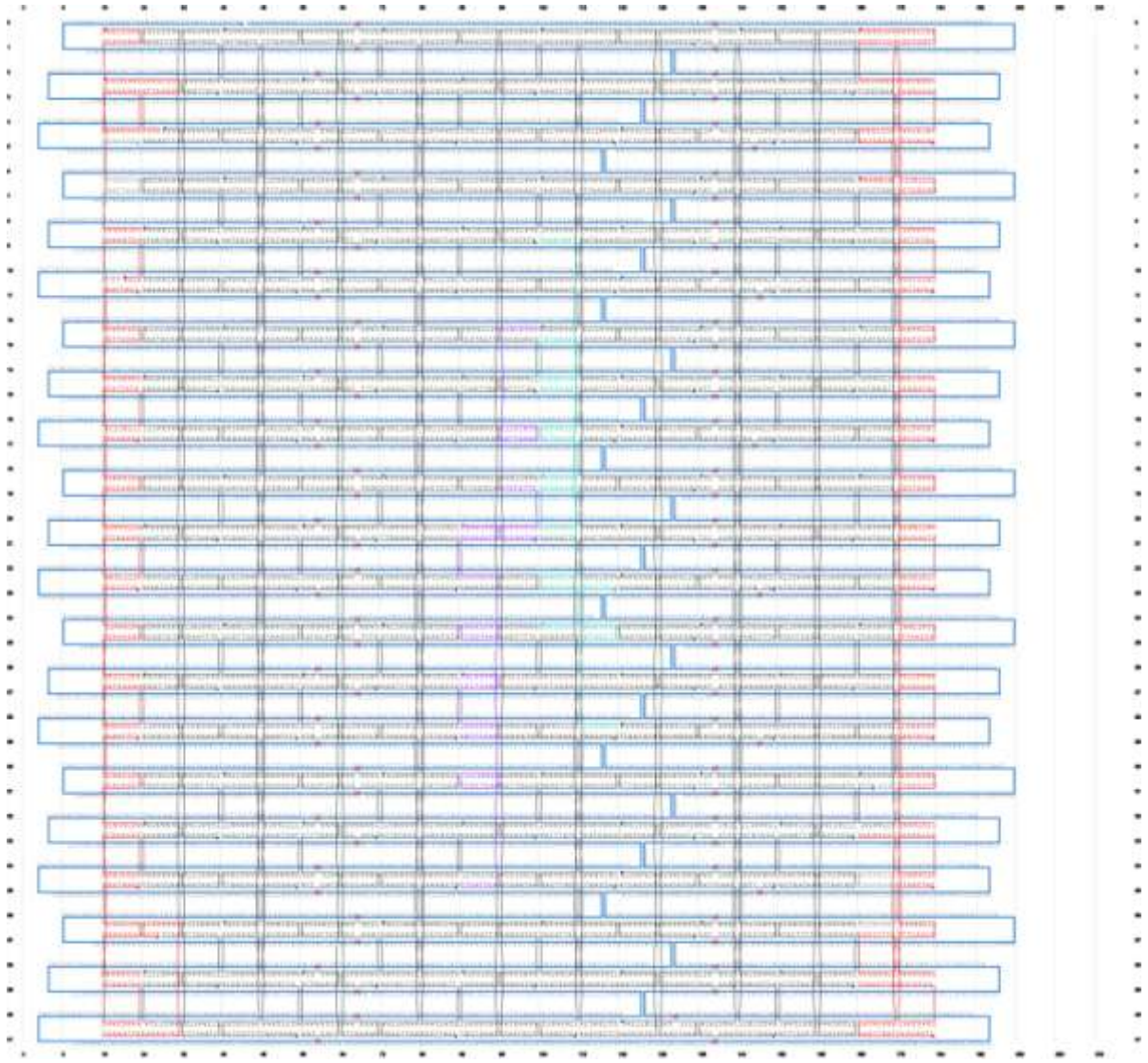

Fig. S1: CaDNAno[4] image of the DNA origami block structure. In the schematic picture the scaffold path (blue), the staple oligonucleotides (grey and red) and the attachment sites (purple and turquoise) are shown. The DNA origami-structure used in between the gold nanoparticles (AuNPs) was a rectangle block of square lattice arranged double helices with the dimensions of 58 nm x 30 nm and a thickness of 8 nm (in solution). Additional information about the details of the structure is described in Stein *et al.*[5]. The DNA origami offers two AuNP attachment sites each consisting of three single-stranded 15xA nucleodite (nt) long extensions on the 3' end of the origami staples. These - in total 6 - extended staple strands are depicted in purple and turquoise color code. By covering the AuNPs with thiol modified single stranded DNA of the complementary sequence to the attachment sites, the AuNPs were bound to the origami structures via DNA hybridization. Here we used 40 nm AuNPs (from BBI solutions) and covered them with 19 nt long 5' thiol modified poly-T DNA strands (biomers.net).

Supporting Figure S2:

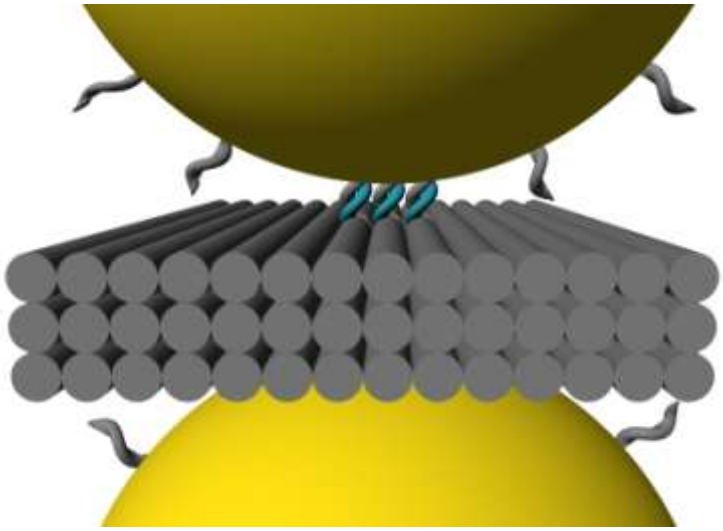

Fig. S2: Scheme of the assembled nanostructure. Double-strands of the DNA origami structure are depicted as grey cylinders. The AuNPs are functionalized with thiol-modified poly-T DNA single strands (grey). Complementary sequences (poly-A, turquoise) branch out at three adjacent points from the DNA origami-structure. Base-pairing of these strands with the strands of the AuNPs leads to the self-assembly of the DNA-based nanoantennas.

Supporting Figure S3:

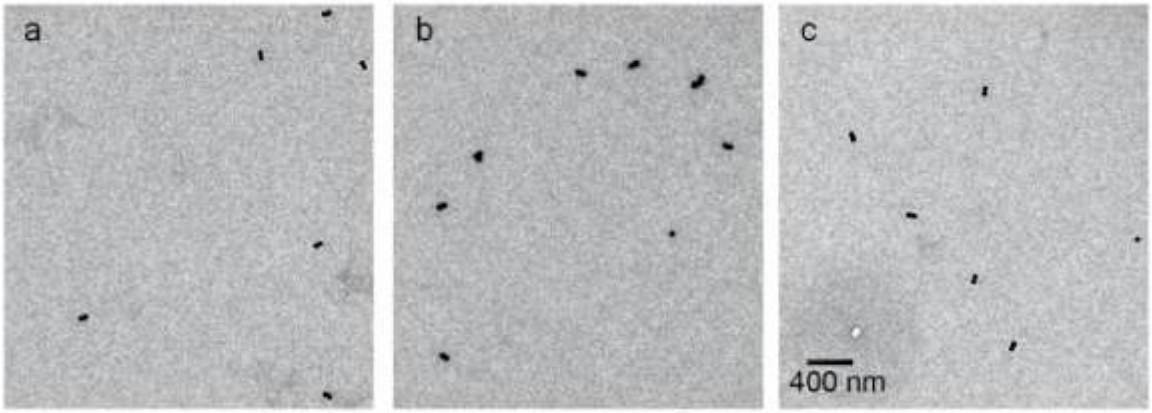

Fig. S3: Wide field TEM images of the nanoantennas. Electron microscopy analysis was used to determine the dimer assembly yield. We observed that up to 72% of the structures analyzed by TEM were correctly assembled dimers. We also found that 20% of the features were individual particles and 8% clusters containing three or more particles. Note that most of the individual particles are not bound to a DNA origami but are instead stray particles that were not incorporated into any structure. Almost all DNA structures have two particles attached.

Supporting Figure S4:

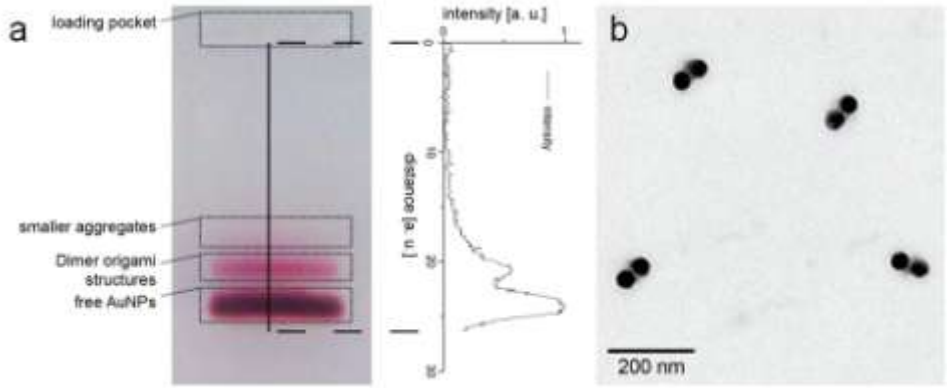

Fig. S4: Purificaton of the DNA Origami nanoantennas from free AuNPs by gel electrophoresis. Gel analysis allows an estimate of the amount of material that folded into structures of desired shape. Some aggregates of DNA structures and gold particles are recognizable as smear (17%), one band with smaller aggregates (13%), one band containing the DNA-assembled gold particle dimers (70%) and one strong band containing the excess of gold particles that are present during folding (not counted) are visible. The dimer band is extracted and the purified structures are used for the measurements.

Supporting Figure S5:

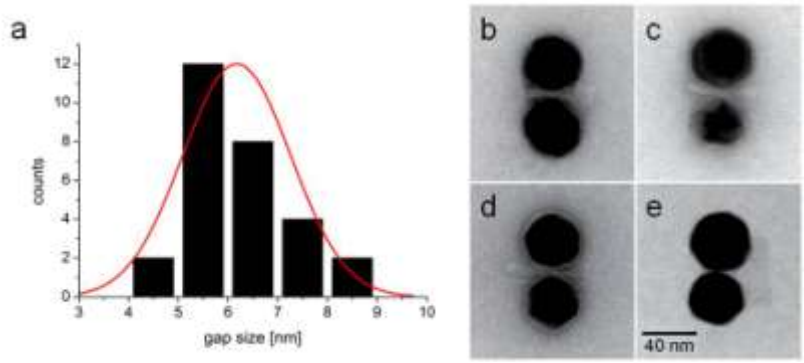

Fig. S5: Statistics of the nanogap size. Measuring the gold particle separation (surface-to-surface) of 28 dimers revealed an average distance of 6 ±1 nm. Note that we excluded dimers with distorted geometry from our measurements. Such distortions can occur during the adsorption and drying process of the structures on the TEM grids. An example for such a distorted object is shown in panel e). Instead of being upright between the two particles, the DNA origami sheet has landed on one side which forced the gold particles into a configuration where their surfaces are almost touching. Out of 40 examined dimers, 12 were excluded for this reason.

Supporting Figure S6:

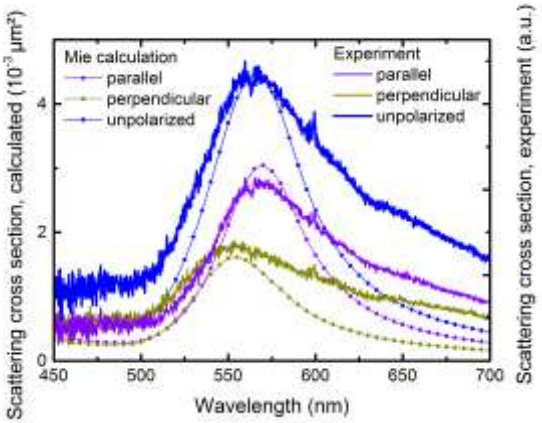

Fig. S6: Comparison between the polarization dependent scattering cross section with Mie calculations. The peak maxima were located at 553 nm for perpendicular and 570 nm for parallel light polarization. The diameter and the gap size in the calculation are 40 nm and 6.8 nm, respectively, which is within the gap size distribution found by TEM measurements (nanoparticle diameter 40 ±3 nm, gap size 6 ±1 nm). The coating of the Au nanoparticles was approximated as a 3 nm layer with a refractive index of 2.1 and the glass/air interface modeled as an effective surrounding medium with a refractive index of 1.35. Convergence was reached when taking a maximum multipolar order of 4 into account. (Calculations were performed with the program 'MQMie' version 3.2a by Dr. Michael Quinten)

Supporting Figure S7:

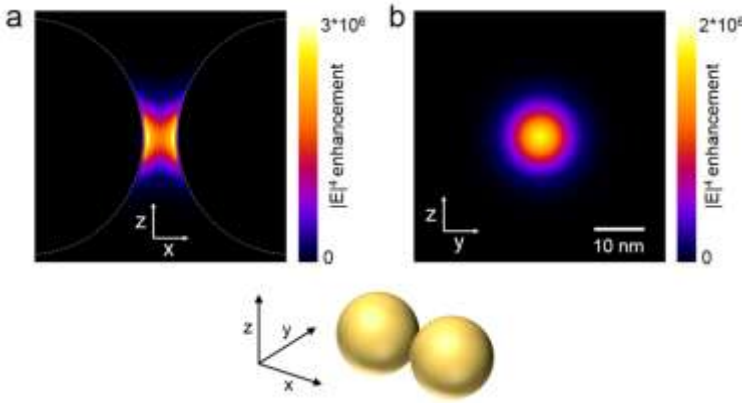

Fig. S7: Finite difference time domain (FDTD) calculations of the $|E|^4$ enhancement in the gap of an Au nanoparticle dimer (sphere diameter 40 nm, gap size 6 nm), evaluated at a wavelength of 570 nm. The incident light was polarized along the dimer long axis (x-direction). The strongest enhancement is observed in the central gap region of 12x6 nm² along the axis of the nanoparticle dimer. The calculations yield a $|E|^4$ enhancement of $1.4 * 10^5$ averaged and a maximum enhancement of $3 * 10^6$ over the hot spot which agrees well with the estimated SERS enhancement. . a) Side-view monitor of the nanoparticle gap, centered at the gap center (i.e. the symmetry point of the dimer). b) Monitor perpendicular to the long dimer axis, centered at the gap center.

Supporting Figure S8:

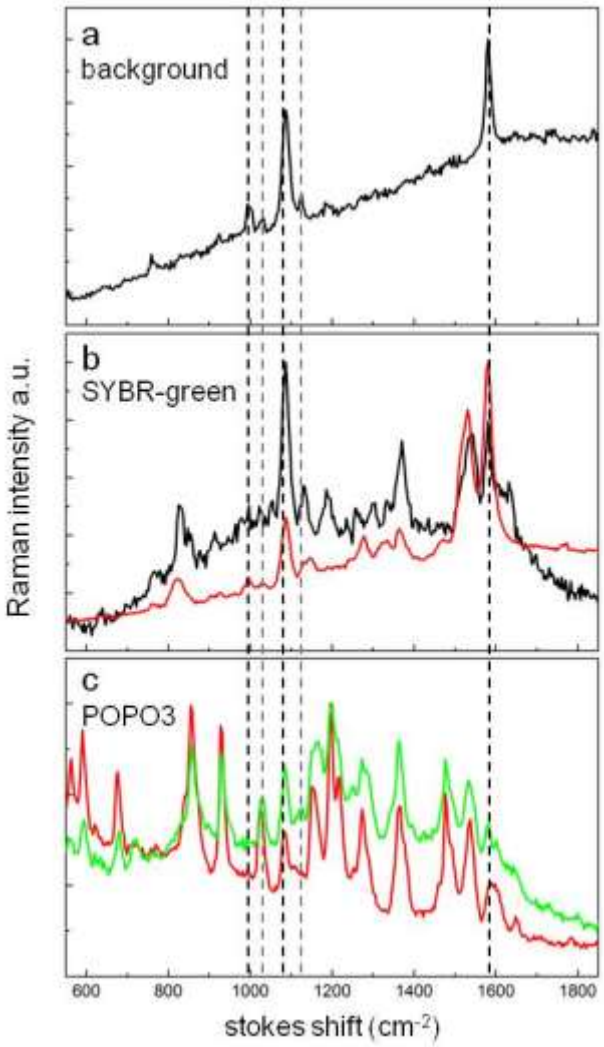

Fig. S8: a) SERS background measured for a plain DNA origami structure. The main peaks are located at 998 cm^{-1}, 1087 cm^{-1}, and 1581 cm^{-1} which is corresponding to the ssDNA coating with a 19nt Thymine sequence, the DNA phosphate backbone, and the complementary Adenine binding to the poly-T strand[6,7,8]. b), c) Comparison of the background signal with SERS spectra of additional DNA label SYBR-green (please see Ref. 3 for the chemical structure) and POPO-3 Iodide (please see Ref. 9 for the chemical structure). Two example spectra are shown from two different dimers. All spectra were measured for a laser intensity of ~ 9 kW/cm^2 and an integration time of 100s.

Supporting Figure S9:

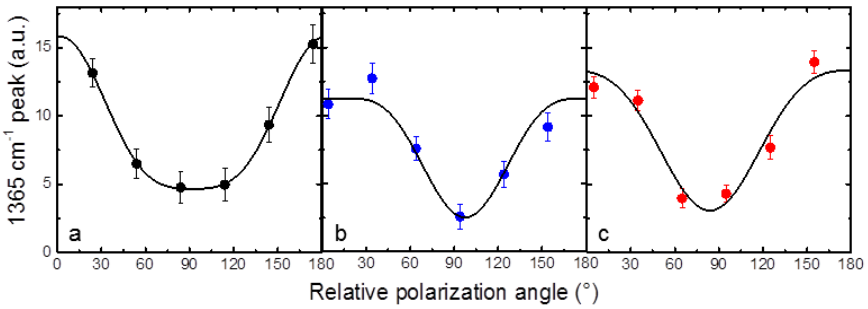

Fig. S9: Fitting of the polarization dependence of the 1365 cm^{-1} peak intensity. Data is fitted with the function $I_{SERS} \sim I^{\perp} cos^4(\alpha + \alpha_0) + I^{||} cos^2(\alpha + \alpha_0) sin^2(\alpha + \alpha_0)$, where α is the angle between the excitation light polarization and the dimer axis. α_0 was set as a fitting parameter in the range of the measurement uncertainty (±7°). $I^{\perp}$ and $I^{||}$ depend on the orientation of the associated Raman dipole of the analyte with respect to the dimer axis. If $I^{\perp}$=0 and $I^{||}$ is maximum, all Raman dipoles in the plasmonic 'hot spot' are aligned with the enhanced electric field, i.e. in this case with the dimer axis. Accordingly, a maximum $I^{\perp}$ and $I^{||}$ =0 represents the case of perpendicular orientation. a) $I^{\perp}$= 13.3 ±7.5, $I^{||}$=112 ±2; b) $I^{\perp}$= 185 ±77, $I^{||}$=87 ±18; c) $I^{\perp}$= 160 ±77, $I^{||}$=103 ±18.

References:

1. Fan, J. A. et al. Self-Assembled Plasmonic Nanoparticle Clusters. Science 328, 1135–1138 (2010).

2. Zhang, X., Servos, M. R. & Liu, J. Instantaneous and Quantitative Functionalization of Gold Nanoparticles with Thiolated DNA Using a pH-Assisted and Surfactant-Free Route. J. Am. Chem. Soc. 134, 7266–7269 (2012).

3. Zipper, H., Brunner, H., Bernhagen, J. & Vitzthum, F. Investigations on DNA intercalation and surface binding by SYBR Green I, its structure determination and methodological implications. Nucleic Acids Res. 32, e103 (2004).

4. Douglas, S. M. et al., Rapid prototyping of 3D DNA-origami shapes with caDNAno. Nucleic. Acid Research 37, 5001-5006 (2009).

5. Stein, I. H., Schüller, V., Böhm, P., Tinnefeld, P. and Liedl, T. Single-Molecule FRET Ruler Based on Rigid DNA Origami Bks. ChemPhysChem, 12, 689 – 695 (2011).

6. Pye, C. C. & Rudolph, W. W. An ab Initio, Infrared, and Raman Investigation of Phosphate Ion Hydration. J. Phys. Chem. A 107, 8746–8755 (2003).

7. Movileanu, L., Benevides, J. M. and Thomas, G. J., Temperature dependence of the raman spectrum of DNA. Part I—Raman signatures of premelting and melting transitions of poly(dA–dT) poly(dA–dT). J. Raman Spectrosc. 30, 637–649 (1999).

8. Barhoumi, A., et al. Surface-Enhanced Raman Spectroscopy of DNA. J. Am. Chem. Soc. 130, 5523–5529 (2008).

9. Zarkov, A., et al. Novel Fluorescent Dyes for Single DNA Molecule Techniques. Mol. Imaging., 12 (2), 90-99 (2013).